ELSEVIER

Chemical Engineering and Processing 35 (1996) 11–19

Chemical Engineering and Processing

Modelling of a trickle-bed reactor II. The hydrogenation of 3-hydroxypropanal to 1,3-propanediol

G. Valerius[a], X. Zhu[a], H. Hofmann[a], D. Arntz[b], T. Haas[b]

[a]*Lehrstuhl für Technische Chemie I, Universität Erlangen-Nürnberg, Egerland-Str. 3, 91058 Erlangen, Germany*
[b]*Degussa, 63403 Hanau, Germany*

Received 8 August 1994; accepted 3 March 1995

Abstract

1,3-Propanediol can be synthesized by the hydrogenation of 3-hydroxypropanal over a nickel catalyst. The aim of the investigation was to obtain information about the mass transfer and degree of wetting in a trickle-bed reactor. The model for the concentration and temperature profiles in a pilot reactor employed was based on kinetic measurements in an autoclave. Two different approximations of the overall catalyst effectiveness factor were used: (1) the effectiveness factors of dry, half wetted and totally wetted slabs were weighted as proposed by Beaudry, Mills and Dudukovic; (2) a new cylinder shell model was used, leading to one-dimensional mass balance equations inside the porous catalyst particle for all possible values of the external wetting efficiency on the particle scale.

Keywords: Modelling; Trickle-bed reactor; Hydrogenation; 3-Hydroxypropanal; 1,3-Propanediol

1. Introduction

3-Hydroxypropanal (HPA) synthesized by acid catalysis from acrolein and used as a 10 ± 0.5 wt.% aqueous solution was employed in this investigation. The hydrogenation reaction was carried out on a nickel catalyst over the temperature range 308–333 K at a pressure of 20–80 bar. The reaction equations are:

$$\underset{\text{acrolein (AC)}}{H_2C{=}CH{-}CHO} \overset{H_2O}{\rightleftharpoons} \underset{\text{3-hydroxypropanal (HPA)}}{HO{-}CH_2{-}CH_2{-}CHO} \xrightarrow{H_2} \underset{\text{1,3-propanediol (PD)}}{HO{-}CH_2{-}CH_2{-}CH_2OH}$$

Under these operating conditions, possible side-reactions and the reversible reaction between acrolein and HPA play only a moderate role in determining the quality of the product. Hence, the interaction between the reaction kinetics, mass transfer and catalyst wetting can be described by the simple reaction scheme

$$\nu A[\text{gaseous}] + B[\text{non-volatile}] \rightarrow \text{product(I)}$$

where reactant A is hydrogen, reactant B is 3-hydroxypropanal (HPA) and 1,3-propanediol (PDO) is the product. Thus all the model equations, presented in Ref. [1], are applicable to the hydrogenation of HPA. It is assumed that any deviations between the global reaction rate in the trickle-bed reactor and the effective reaction rate in a spinning-basket reactor per mass of catalyst can only arise from three factors: (1) deactivation of the catalyst; (2) partial external wetting of the catalyst; and (3) external mass transfer limitation of hydrogen.

2. Intrinsic kinetics

The intrinsic rate of reaction per mass of catalyst powder in a stirred tank reactor excluding any mass transfer limitation has been adequately described by the following rate equation [2]:

$$r_m = -\frac{dc_B}{c_{cat}\,dt} = \frac{K_1 K_2 k_m\, e^{-E_a/RT} c_B c_A}{(1 + K_1 c_B + K_2 c_A)^2} \quad (1)$$

where

$c_A = c^*_{l,A}$ corresponds to liquid saturated with hydrogen
$c^*_{l,A} \neq f(T)$, in the range 38–60 °C
$c^*_{l,A} \propto p$, where p is the pressure of the pure gas phase (Henry's law)

Table 1
Kinetic parameters and confidence limits for the intrinsic kinetics

b_k	$\beta_k \pm \sqrt{D_{kk}} st_\gamma$
K_1 (l mol^{-1})	13.2 ± 2.5
K_2 (l mol^{-1})	141 ± 28
k_m [mol(g cat)$^{-1}$ s^{-1}]	$5.25 \times 10^6 \pm 1.04 \times 10^6$
E_a (kJ mol^{-1})	65.5 ± 0.6

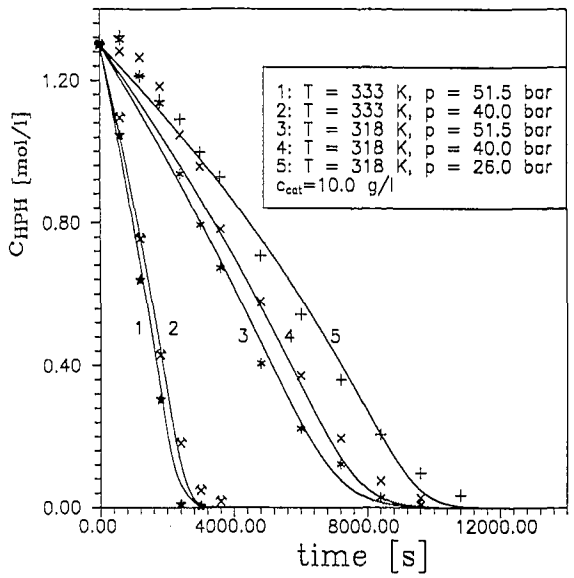

Fig. 1. Kinetic measurements fitted by Eq. (1) using the values of the parameters listed in Table 1.

$c^*_{l,A} \neq f(c_{l,B}, c_{l,P})$ corresponds to the solubility of hydrogen in water
$c^*_{l,A}$ (40 bar) = 0.029 mol l^{-1} [3]

Estimated values of the kinetic parameters and their confidence limits are given in Table 1. In Fig. 1, the measured concentration profiles are described by Eq. (1) using the parameter values given in Table 1[1].

3. Effective kinetics

The same catalyst pellets were used (characteristic length $L_c = V_p/O_p = 0.18$ mm) in the spinning-basket reactor and trickle-bed reactor. As long as excess of

Table 2
Estimated pore diffusion coefficient and tortuosity factor τ

Regression	Parameter
$r_{m,eff} = \eta_p r_m$	$D_{e,A} = 1.1 \times 10^{-5}$ cm^2 s^{-1} respectively $\tau = 2.5$ $D_{e,B} = 2.2 \times 10^{-6}$ cm^2 s^{-1} (estimated from the molecular diffusivity of similar components as HPA)

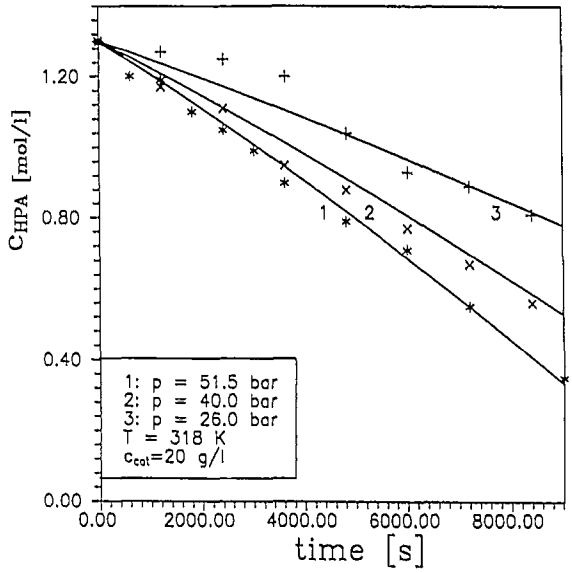

Fig. 2. Effective kinetics described by the model of intrinsic kinetics [Eq. (1) and Table 1] and Bischoff's approximation for the effectiveness factor [Eq. (2) and Table 2].

HPA exists inside the porous catalyst (in the spinning-basket reactor with complete external wetting this can be decided by the criterion $D_{e,B} c_{l,B} \gg D_{e,A} c^*_{l,A}$), Bischoff's approximation [given in Eq. (2)] can be used for the effectiveness factor η_p. Because the measured intrinsic rate is more than three-times higher than the effective rate, it can be assumed that the concentration of hydrogen in the centre of the catalyst is zero.

$$\eta_p = \frac{\left(2D_{e,A}\int_0^{c_{A,s}} \frac{K_1 K_2 k_m \rho_p \, e^{-E_a/RT} c_{s,B} c_A}{(1 + K_1 c_{s,B} + K_2 c_A)^2} \, dc_A\right)^{0.5}}{L_c\left[\frac{K_1 K_2 k_m \rho_p \, e^{-E_a/RT} c_{s,B} c_{s,A}}{(1 + K_1 c_{s,B} + K_2 c_{s,A})^2}\right]} \quad (2)$$

The only unknown parameter in Eq. (2) is the effective pore diffusion coefficient $D_{e,A}$, which can be determined

[1] The confidence limits of the kinetic parameters given in Table 1 must be seen relative to the uncertainty of the parameters employed in the reactor model. This uncertainty results partly from the simplified reaction scheme νA[gaseous] + B[non-volatile] → product, on which the modelling in this investigation is based, and from the analytical error. Some reflections about the wetting parameter f_w will show that the kinetic parameters given above are suitable. The weighting of slabs proposed by Dudukovic and coworkers [4] intuitively gives a good approximation of the reactor-scale and particle-scale incomplete wetting using only one wetting parameter, but nevertheless there is no exact proof of its accuracy. The way to determine the wetting parameter by tracer methods [5–8] intuitively has a closer relationship to the cylinder shell model without consideration for reactor-scale incomplete wetting than the model of weighted slabs. Furthermore, different investigations have shown that for one value of f_w (in the literature often called η_{ce}) deviations in the resulting value of the effectiveness factor η_0 of more than 20% occur if different distributions of the liquid on the outer catalyst surface are presumed [9,10]. For these reasons, the uncertainty in the kinetic parameters seems to be acceptable as a first approximation.

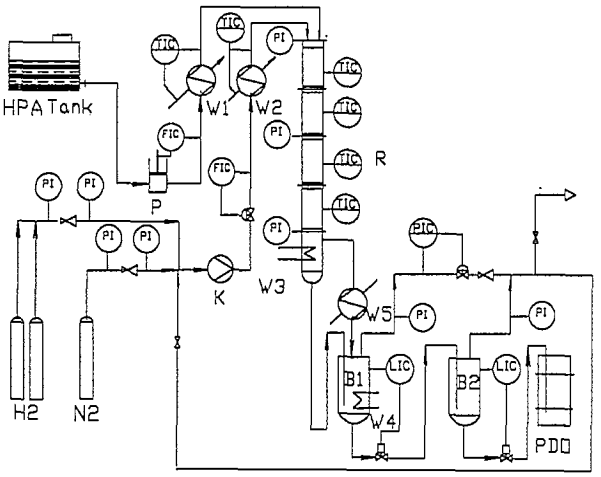

Fig. 3. Simplified scheme for the pilot trickle-bed reactor.

by regression using the models for r_m and η_p and the measured concentration profiles versus time in the spinning-basket reactor. The results are given in Table 2 and Fig. 2.

4. Global kinetics

4.1. The pilot trickle-bed reactor

Fig. 3 shows a simplified scheme for the pilot trickle-bed reactor. The reactor consist of four segments each 146 cm in length with an inner diameter of 7.63 cm. Many temperature and pressure sensors are distributed along the reactor. Each segment is provided with four appliances for taking liquid samples. The aqueous 10 wt.% solution of HPA flows cocurrently with hydrogen through the trickle bed. After separating the gas and liquid, an aqueous solution of 1,3-propanediol is obtained.

4.2. Mass and heat balances for the liquid phase

Mass and heat balances have been used to describe the measured temperature and HPA concentration along the reactor axis. The mass balance of HPA is given by Eq. (3):

$$-u_{0l}\frac{dc_{l,B}}{dz} = a_i\eta_0\rho_s r_m(c^*_{l,A}, c_{l,B}, T) \quad (3)$$

In this equation, a_i is the catalyst activity which has to be introduced since there was a moderate deactivation of the catalyst with time which had to be taken into account.

The mass balance of hydrogen is given in Eq. (4)[2]:

$$k_l a(c^*_{l,A} - c_{l,A}) - u_{0l}\frac{dc_{l,A}}{dz} = a_i\eta^l_0\rho_s r_m(c^*_{l,A}, c_{l,B}, T) \quad (4)$$

In the mass balance of hydrogen, a modified effectiveness factor η^l_0 has been used to consider partial wetting; the upper index l denotes liquid. The global reaction rate $a_i\eta_0\rho_s r_m(c^*_{A,l}, c_{B,l}, T)$ is equal to the consumption of hydrogen, which in turn is equal to the whole diffusion flux per time of hydrogen through the outer surface of the catalyst particles; the term $a_i\eta^l_0\rho_s r_m(c^*_{A,l}, c_{B,l}, T)$ is equal to the diffusion rate from *flowing liquid* through the outer catalyst surface. For complete wetting, η^l_0 is equal to η_0. The mass balances which lead to the exact definition of η^l_0 are given in Ref. [1].

The heat balance of the liquid phase is given by Eq. (5):

$$-u_{0l}\rho_l c_p\frac{dT}{dz} = a_i\eta_0\rho_s r_m(c^*_{l,A}, c_{l,B}, T)\,\Delta H_R \quad (5)$$

The values for water were used for the specific heat c_p and the density of the liquid phase ρ_l of the solution (containing 10 wt.% HPA). For a complete conversion of 1.3 mol HPA l^{-1}, a temperature rise in the trickle-bed reactor of about 19 K was measured. Assuming adiabatic conditions, the heat of reaction ΔH_R can be estimated from:

$$\Delta H_R = \frac{\Delta T_{ad}\rho_l c_p}{c_{l,B}} \approx \frac{-19\text{ K} \times 0.97\text{ kg l}^{-1} \times 4.2\text{ kJ mol}^{-1}}{1.3\text{ mol l}^{-1}}$$
$$= -60\text{ kJ mol}^{-1} \quad (6)$$

The difference between the heat of formation of 1-propanol and propionaldehyde $\Delta H \approx -66$ kJ mol^{-1} [11] can be used as an approximation for the heat of reaction, indicating that the assumption of adiabatic conditions appears to be correct.

All the kinetic parameters for the hydrogenation of HPA are summarized in Tables 1–3.

4.3. Solid-phase mass balances for the model of weighted slabs [1]

The mass balances for an infinite catalyst slab are given in Eqs. (7) and (8):

$$D_{e,A}\frac{dc^2_A}{dx^2} = a_i\rho_p r_m(c_A, c_B) \quad (7)$$

$$D_{e,B}\frac{dc^2_B}{dx^2} = a_i\rho_p r_m(c_A, c_B) \quad (8)$$

Table 3
Kinetic parameters

ΔH_R (kJ mol^{-1})	−60
ρ_s (g l^{-1})	800
ρ_p (g l^{-1})	1330

[2] The whole external mass-transfer resistance of the gas is assumed to be on the liquid side of the gas/liquid-film, as proposed in Ref. [1].

As shown in Ref. [1], there are three possibilities for calculating the effectiveness factor of a single particle, and in each case two may be used to control the numerical solution. Only one example is given here.

The effectiveness factor η_{hw} of a half-wetted infinite slab, which is dry at $x = 0$ and wetted at $x = 2L_c$, can be calculated from Eq. (9):

$$\eta_{hw} = \frac{D_{e,B}\left.\frac{dc_B}{dx}\right|_{x=2L_c} \frac{A_p}{2}}{V_p a_i \rho_p r_m(c^*_{l,A}, c_{l,B})} = \frac{D_{e,B}\left.\frac{dc_B}{dx}\right|_{x=2L_c}}{2L_c a_i \rho_p r_m(c^*_{l,A}, c_{l,B})} \quad (9)$$

For calculating the overall effectiveness factor, the effectiveness factors for the half-wetted and totally wetted slabs are calculated and weighted as proposed by Dudukovic [Eq. (10)][3]:

$$\eta_0 = f_w^2 \eta_{cw} + 2(1 - f_w) f_w \eta_{hw} + (1 - f_w)^2 \eta_{nw} \quad (10)$$

4.4. Solid-phase mass balances for the cylinder shell model

The mass balances for a cylinder shell are given by Eqs. (11) and (12) [1]:

$$D_{e,A}\left(\frac{d^2c_A}{dx^2} + \frac{1}{x} \cdot \frac{dc_A}{dx}\right) = a_i \rho_p r_m(c_A, c_B) \quad (11)$$

$$D_{e,B}\left(\frac{d^2c_B}{dx^2} + \frac{1}{x} \cdot \frac{dc_B}{dx}\right) = a_i \rho_p r_m(c_A, c_B) \quad (12)$$

Here, the overall effectiveness factor is equal to the effectiveness factor of the cylinder shell, which can be calculated for example from the diffusion flux of hydrogen through the wetted surface at $x = R_A$ and through the unwetted surface at $x = R_i$:

$$\eta_0 = \frac{D_{e,A}\left(\left.\frac{dc_A}{dx}\right|_{x=R_a} A_a - \left.\frac{dc_A}{dx}\right|_{x=R_i} A_i\right)}{V_p a_i \rho_p r_m(c^*_{l,A}, c_{l,B})}$$

$$= \frac{D_{e,A}\left(\left.\frac{dc_A}{dx}\right|_{x=R_a} f_w - \left.\frac{dc_A}{dx}\right|_{x=R_i} (1 - f_w)\right)}{L_c a_i \rho_p r_m(c^*_{l,A}, c_{l,B})} \quad (13)$$

4.5. Numerical solution of the model equations

The numerical solution of the model equations starts with the single pellet mass balances at the beginning of the catalyst packing. For the balance equations relating to diffusion and reaction in the pores of the catalyst, a discretization by central differences (12–80 interpolation nodes) was made and the resulting system of non-linear equations was solved by Newton–Kantorowitch's method (4–10 iterations were necessary). After calculation of the required effectiveness factors, the mass and heat balances of the flowing liquid [Eqs. (3)–(5)] were solved by forward integration; the single-pellet mass balances had each to be solved for $\Delta z = 5$ cm while integrating Eqs. (3)–(5) from the beginning to the end of the catalyst packing, because η_0 varies with the temperature and with the concentrations of the reactants.

4.6. Experimental results and model predictions

4.6.1. The different experimental series

Three series of experiments under trickle-bed operation were carried out. In the first and second experimental series, the catalytic activity was in the same range and about two-times higher than in the third series.

It was necessary to investigate the effect of temperature on the global reaction rate in a laboratory trickle-bed reactor (first experimental series) before experiments in the pilot plant were commenced. The results may be expressed in the form of an apparent activation energy $E_{app} = 12$ kJ mol^{-1}.

The second experimental series was carried out in the pilot trickle-bed reactor described above to determine the effect of liquid superficial velocity u_{0l} on the global reaction rate. Some results from these experiments will be described later together with the predictions of the reactor model. As a result of these experiments, an increase in the global reaction rate with increasing u_{0l} was established.

Unfortunately there was a considerable loss of catalytic activity between the second and the third experimental series. Thus, after the experiments had been completed, it was found by AAS analysis that the catalyst pellets had lost nickel, possibly as a result of acids formed in the HPA aqueous solution. Hence the third experimental series was not suitable for modelling. Nevertheless, the pressure dependence of the reaction studied in the third series — expressed by an 'order n_p', i.e.

$$\frac{r_{g,50\%}(80\text{ bar})}{r_{g,50\%}(40\text{ bar})} = \left(\frac{80\text{ bar}}{40\text{ bar}}\right)^{n_p}$$

— was close to zero rather than unity. However, unpublished experimental results on the hydrogenation of xylose in aqueous solution using a pilot plant in this laboratory indicate a similar effect concerning the influence of reactor pressure on the global reaction rate, although simulations indicated an external mass-transfer limitation of hydrogen. Hence the pressure-dependence of a gas-limited reaction seems to be significantly lower than that predicted by modelling using correlations for $k_l a$ and f_w from the literature.

[3] The effectiveness factor of a completely unwetted slab is zero because there is no HPA in the slab.

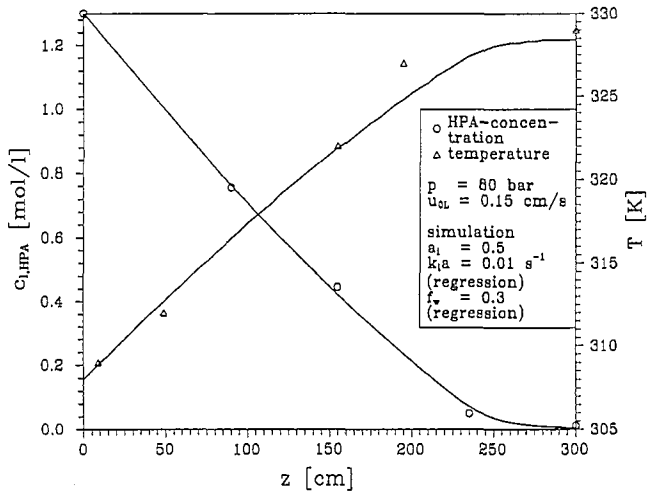

Fig. 4. Fitting the model to the measured concentration and temperature profiles.

4.6.2. Determination of the parameters of the reactor model

The parameter with the greatest uncertainty in the reactor model is the degree of catalyst deactivation a_i. Observation of the activity of the catalyst under trickle-bed operation and repeating experiments in the spinning-basket reactor gave some idea of the degree of deactivation, but no exact value for a_i could be obtained. The first value of $a_i = 0.5$ was obtained by fitting the model to the experimental results[4].

As discussed later, this value of a_i is confirmed by the temperature-dependence of the global reaction rate.

For the determination of the parameters k_la and f_w, three different possibilities exist: (1) simultaneous fitting of the global model to the measured $(c_B, T) = f(z)$ profiles; (2) evaluation of correlations for k_la and f_w given in the literature; and (3) modelling of an ideal trickle-bed reactor with $k_la = \infty$ and $f_w = 1$.

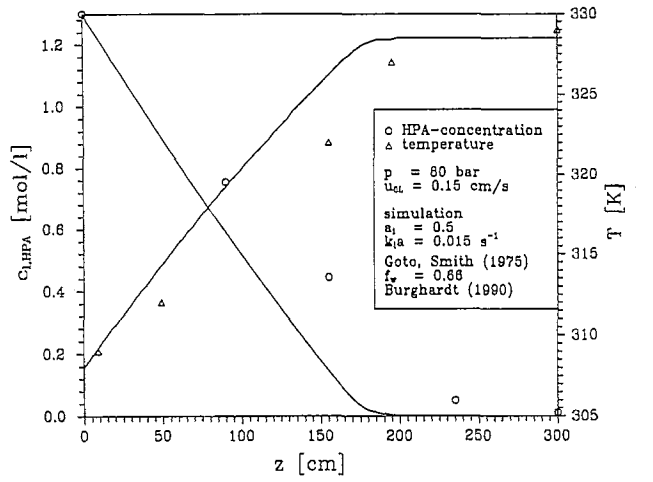

Fig. 5. Predictions of the model (using correlations from the literature) and measured concentration and temperature profiles.

Measured concentration and temperature profiles and model predictions

In Fig. 4 the reactor model has been fitted to the measured concentration and temperature profiles in the trickle-bed reactor while in Fig. 5 correlations given in the literature have been used in the model equations (overall effectiveness factor calculated from the model of weighted slabs)[5,6].

Fig. 6 shows that the global reaction rate is greatly overpredicted by the model of an ideal trickle-bed reactor[7]. At this point it could be advanced that a better description of the measurement can possibly be

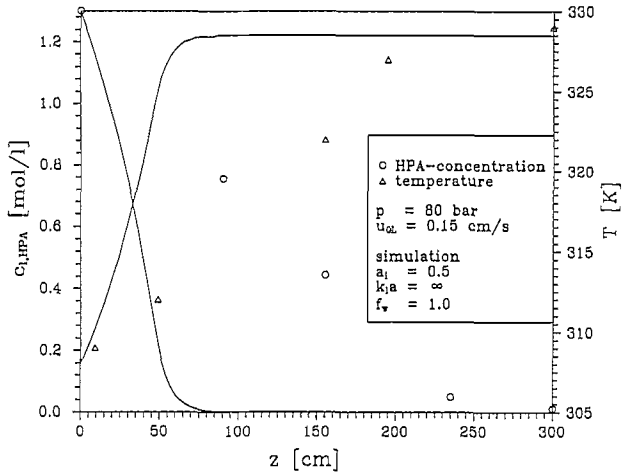

Fig. 6. Modelling of an ideal trickle-bed reactor and measured concentration and temperature profiles.

[4] Fitting the three model parameters a_i, k_la and f_w to the three experimental runs taken from the second experimental series (with three different liquid superficial velocities) resulted in approximately the same value for a_i. For these calculations, the model of weighted slabs as proposed by Dudukovic and coworkers was used.

[5] Better agreement between simulation and measurement with the parameter value $f_w = 0.3$ (Fig. 4) than with the parameter value $f_w = 0.66$ (Fig. 5) must not be interpreted as indicating that Burghardt's correlation is wrong. There is a great uncertainty in the simultaneous determination of three parameters from only one measured $(c_B, T) = f(z)$ profile.

[6] The formation of a new correlation requires the consideration of more than one measurement. The use of $(c_B, T) = f(z)$ profiles measured at different pressures would be best for this purpose, because the parameter values should be nearly independent of the reactor pressure. However, the first aim of the experiments (second experimental series) was to analyze whether there was a local maximum in the global reaction rate in its dependence on the liquid superficial velocity. Because the experiments in the pilot plant required large amounts of material (2000 l of HPA solution were consumed) and work time, the investigations had to be completed with the third series. Hence the aim of the present investigation was not to give a new correlation for the wetting efficiency, f_w.

[7] The 'ideal trickle-bed reactor' is defined in Ref. [1].

obtained by reducing the factor a_i in the model of an ideal trickle-bed reactor. But this objection may be rejected by analyzing the influence of the operational parameters on the global reaction rate. If the assumptions leading to the model of an ideal trickle-bed reactor are right, then the apparent activation energy E_{app} in the trickle-bed reactor would have to be in the range of $E_a/2$ to E_a (E_a is the activation energy of the intrinsic kinetics given in Table 1); in fact a value of $E_{app} = 12\ kJ\ mol^{-1}$ was measured and not $E_a = 33–66\ kJ\ mol^{-1}$.

4.6.3. Significance of the parameters of the reactor model

From the decrease in the global reaction rate in trickle-bed operation together with the loss of nickel from the catalyst, it can be concluded that a_i is a significant parameter in the reactor model. From the temperature-dependence ($E_{app} < E_a/2$), it can be concluded that in addition to the inner mass-transfer limitation of hydrogen (which has already been established in the spinning-basket reactor) in trickle-bed operation, there must be a further mass-transfer resistance: partial external wetting or stagnant liquid pockets possibly lead to an increased mass-transfer resistance for HPA and the external liquid film possibly offers a significant mass-transfer resistance for hydrogen.

As reported above, the experimental results obtained at different temperatures can be expressed by an apparent activation energy $E_{app} = 12\ kJ\ mol^{-1}$. Evaluating the change in the calculated global reaction rate with temperature gives a result which can also be expressed by an apparent activation energy. With $a_i = 0.5$, different combinations of $(k_l a; f_w)$ can approximate the measured global reaction rate and — neglecting the temperature-dependence of the diffusivity — all these combinations result in an apparent activation energy $E_{app} \approx 9\ kJ\ mol^{-1}$. Hence, if we assume in addition a slight temperature-dependence of the diffusivity, the response to temperature change in the model and in the experiment agree well. These calculations confirm the value of $a_i = 0.5$, but they give no information as to whether the decrease in the temperature-dependence in the trickle-bed reactor relative to the rotating-basket reactor is caused by an increased mass-transfer resistance of hydrogen, of HPA or of both reactants.

For liquid superficial velocities $u_{0l} = 0.12–0.48\ cm\ s^{-1}$, as used in the second experimental series, correlations for external wetting efficiency in the literature give values in the range $f_w = 0.6–1.0$ [12]. If these values for f_w are correct, it can be concluded that for the highest liquid velocity the catalyst is nearly completely wetted externally so that hydrogen is the only limiting reactant, while at lower liquid velocities both reactants are limiting. Using a weighted multi-response regression employing the model of weighted slabs and

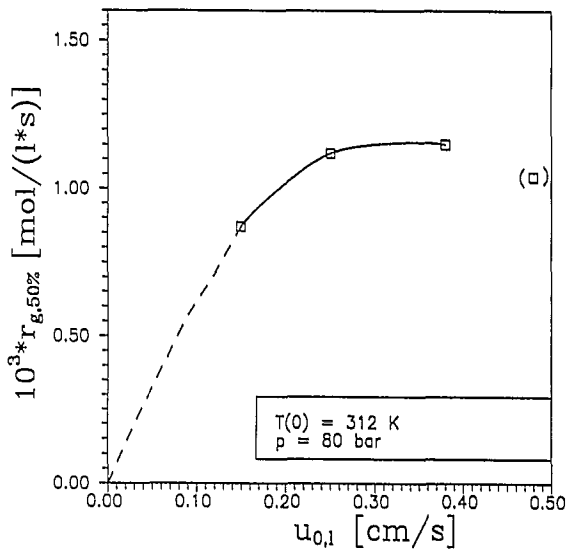

Fig. 7. Global reaction rate in the hydrogenation of 3-hydroxypropanal.

the measured $(c_{l,B}, T) = f(z)$ profiles in the trickle-bed reactor, values of $f_w = 0.3–0.6$ were obtained. As mentioned above, such a regression cannot be very reliable since neither the reactor pressure nor the initial conditions were varied in the experiments reported here. Nevertheless, an initial indication of lower external wetting efficiencies than given in the literature arises, which seems to be confirmed by some of the following considerations.

In the discussion concerning the activity a_i given above, the responses to changes in temperature in the reactor and in the reactor model were compared. In the following explanations, attempts will be made to obtain information about $k_l a$ and f_w in a similar manner, i.e. for different combinations $(k_l a, f_w)$, the response of the model to changing the operational parameters u_{0l} and p will be analyzed and compared with the experimental results from the trickle-bed reactor.

Fig. 7 shows the average global reaction rate for a conversion of 50% for different liquid space velocities. In the first experimental series in the laboratory reactor, as u_{0l} increased an increase in $r_{g,50\%}$ occurred (dashed line). Increasing the liquid space velocity from $0.12\ cm\ s^{-1}$ to $0.24\ cm\ s^{-1}$ gave an additional significant increase in the reaction rate. The further increase of u_{0l} from $0.24\ cm\ s^{-1}$ to $0.36\ cm\ s^{-1}$ led to only a moderate increase in $r_{g,50\%}$. The lower value of $r_{g,50\%}$ at $u_{0,l} = 0.48\ cm\ s^{-1}$ has been placed in brackets because all attempts to reproduce it failed. A strong increase in the pressure drop while increasing u_{0l} in the range $0.45–0.50\ cm\ s^{-1}$, interpreted as corresponding to transition from the low interaction regime to the high interaction regime, led to unstable operation of the reactor which was very sensitive to slight variations in the liquid velocity.

The correlation between the global reaction rate and the liquid velocity agrees well with Satterfields findings in different reaction studies. On initial inspection only the very uncertain value of $r_{g,50\%}$ at $u_{0l} = 0.48$ cm s^{-1} agrees with Herskowitz' theory of improved mass transfer with decreasing u_{0l} relative to f_w for a gas-limited reaction. However, it should not be concluded at this point that Herskowitz' theory might be wrong, because it is also possible here that the non-volatile reactant HPA becomes limiting on decreasing u_{0l} relative to f_w.

In Fig. 8 the overall effectiveness factor is plotted against the external wetting efficiency using estimated mean values for the temperature and the HPA and hydrogen concentrations. For complete external wetting, the only difference between both models is the geometry of the catalyst. The consideration of reactor-scale partial wetting in the model of weighting slabs generally leads to smaller values of η_0 in this model than in the cylinder shell model. Partial wetting on the particle scale results in a higher catalyst effectiveness than partial wetting on the reactor scale; thus the cylinder shell model gives the higher maximum of $\eta_0 = f(f_w)$.

No indications allowing further analysis of the problem — including the parameter $k_l a$ [8] — with respect to a possible maximum in the reaction rate were found. Nevertheless the combination of Figs. 7 with 8 leads to the suggestion of lower wetting efficiencies in the experiment than those given in literature [6,12,13].

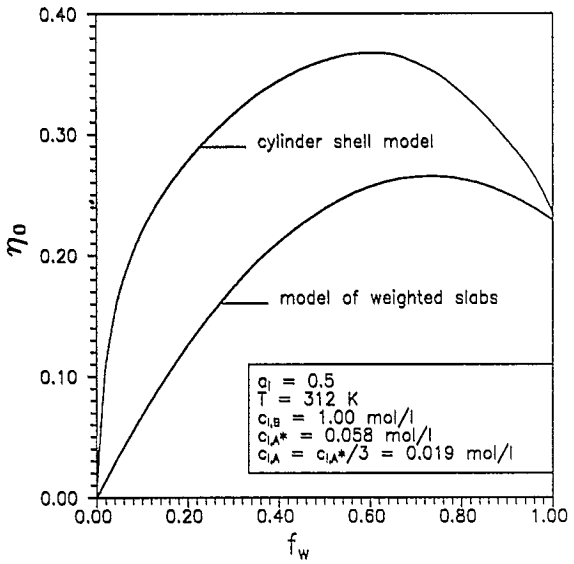

Fig. 8. The overall effectiveness factor for different wetting models.

[8] Although $k_l a$ — determined by ab- and de-sorption experiments — increases with increasing u_{0l} (relative to f_w), it cannot be concluded that the flowing liquid is more saturated with hydrogen at higher liquid rates since (1) $k_l a$ is based on the volume of the packing and (2) $k_l a$ is related to a model assuming complete external wetting [14].

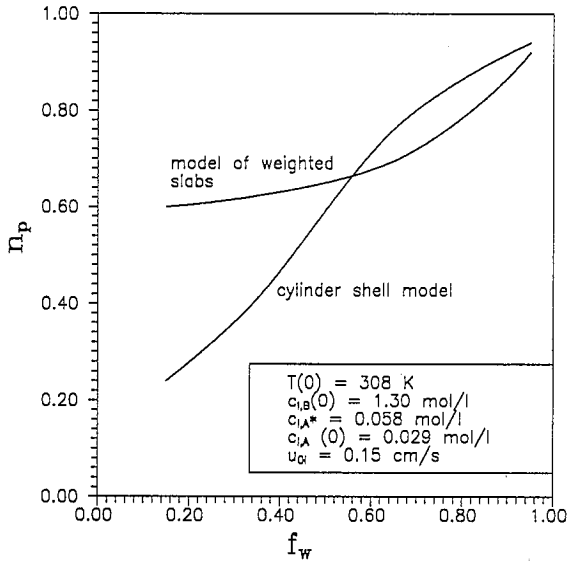

Fig. 9. The effect of external catalyst wetting on the reaction order relative to the pressure (simulation).

The pressure-dependence also confirms the possibility of smaller wetting efficiencies than those quoted in the literature. As illustrated in Fig. 9, the order n_p associated with the reactor pressure decreases with decreasing values of f_w in the model, since the diffusivity of HPA becomes limiting. Values of n_p close to zero — as found experimentally — can only be obtained via the cylinder shell model using wetting efficiencies less than those given in the literature.

5. Conclusions

Two different approximations of the overall catalyst effectiveness factor have been used for modelling the hydrogenation of 3-hydroxypropanal. Both approximations, i.e. the model of weighted slabs and the cylinder shell model, have two common advantages: (1) the problem of partial external wetting is considered using only one parameter and (2) the single-pellet mass balances are one-dimensional, which is very helpful in the case of non-linear bimolecular reaction kinetics and non-isothermal conditions where the overall effectiveness factor η_0 depends strongly on the axial coordinate z.

When compared with the model of weighted slabs, the cylinder shell model has the advantage that incomplete external wetting on the particle scale is not restricted to $f_w = 0.5$. On the other hand, the model of weighted slabs also considers in an intuitively realistic way the problem of incomplete external wetting on the reactor scale. In the cylinder shell model, the same average wetting characteristics are assumed for all particles.

In the hydrogenation of 3-hydroxypropanal, mass transfer of the gas through an outer liquid film and partial external wetting of the catalyst seem to affect the global reaction rate. In both models mentioned above,

parameter values of $f_w = 0.6–1.0$ would lead to a higher pressure dependence and, on increasing the liquid superficial velocity, to a maximum in the global reaction rate, which has yet to be observed experimentally. Better agreement between the response of the model and experimental observations on changing the operational parameters may be obtained by assuming lower values of f_w, so that pore diffusion of 3-hydroxypropanal limits the reaction rate. Calculations with the cylinder shell model show that a low wetting efficiency on the particle scale leads to a low pressure dependence, as found experimentally.

As long as the ideal trickle-bed reactor remains to be verified for a reaction not limited by the gaseous reactant, and as long as the maximum of the reaction rate as a function of liquid velocity for a gas-limited reaction has not been verified experimentally, there remains a certain doubt regarding the attainment of complete external wetting at high liquid rates. This statement concerns wetting as a contact between flowing liquid ('liquid phase') and liquid trapped in the pores ('solid phase'). When industrial workers report complete wetting in their trickle-beds, they often have in mind the fact that they did not find any dry particles after opening their reactor.

Nomenclature

a_i activity factor; ratio of activity of catalyst in the trickle-bed reactor to the activity of fresh catalyst used in the rotating basket reactor, –

a_p external surface of catalyst particles per unit volume of packing, cm^{-1}

A_a external surface of a cylinder shell, cm^2

A_i inner surface of a cylinder shell, cm^2

A_p external surface of a catalyst pellet, cm^2

A_{nw} external not wetted surface of a catalyst pellet, cm^2

A_R reactor cross-section, cm^2

c_j concentration of component j (j = A, hydrogen; j = B, HPA; j = P, 1,3-propanediol) inside the catalyst pellet, $mol\ l^{-1}$

c_p heat capacity, $kJ\ g^{-1}\ K^{-1}$

$c_{cat,1}$ mass of catalyst per volume of liquid in the stirred tank reactor, $g\ l^{-1}$

$c_{cat,2}$ mass of catalyst per volume of liquid in the spinning basket reactor, $g\ l^{-1}$

$c_{cat,3}$ mass of catalyst per volume of liquid in the trickle-bed reactor, $g\ l^{-1}$

$c_{l,j}$ concentration of component j in the external liquid, $mol\ l^{-1}$

$c^*_{l,A}$ saturation concentration of reactant A, $mol\ l^{-1}$

C_1, C_2 integration constants, –

$D_{e,j}$ pore diffusion coefficient of component j, $cm^2\ s^{-1}$

D_{app} apparent pore diffusion coefficient, $cm^2\ s^{-1}$

E_a activation energy of the intrinsic kinetics, $kJ\ mol^{-1}$

E_{app} activation energy of the global kinetics, $kJ\ mol^{-1}$

ΔH_R reaction enthapy, $kJ\ mol^{-1}$

f_w external wetting coefficient, –

K_j constants in the intrinsic rate equation, $l\ mol^{-1}$ (in a mechanistic interpretation — which is not relevant for this investigation — K_j would be equal to the adsorption constant of component j)

$k_l a$ mass-transfer coefficient from gas to liquid based on the volume of catalyst packing, s^{-1}

k_m reaction rate constant based on mass of catalyst, $mol\ (g\ cat)^{-1}\ s^{-1}$ [or $l\ (g\ cat)^{-1}\ s^{-1}$ depending on the rate equation]

L distance between centre and outer surface of catalyst pellet, cm

L_c characteristic length V_p/A_p of a catalyst pellet, cm

L_r reactor length, cm

n_p order of global kinetics relative to reactor pressure, –

O_{cs} external surface area of a cylinder shell, cm^2

O_p external surface area of a single catalyst pellet, cm^2

R_a outer radius of a cylinder shell, cm

R_i inner radius of a cylinder shell, cm

r_g global rate of reaction based on volume of catalyst packing, $mol\ g\ cat^{-1}\ s^{-1}$

$r_{g,X}$ average global rate of reaction based on volume of catalyst packing, $mol\ l^{-1}\ s^{-1}$

r_m intrinsic rate of reaction based on mass of catalyst, $mol\ l^{-1}\ s^{-1}$

T temperature, K

u_{0l} liquid superficial velocity, $cm\ s^{-1}$

V_p volume of a single catalyst pellet, cm^3

V_R volume of the reactor, cm^3

V_{cs} volume of a cylinder shell, cm^3

x coordinate inside the catalyst, cm

X conversion of reactant B

z coordinate in the axial direction of the reactor, cm

ϕ Thiele modulus of a cylinder shell, –

ϕ_p generalized Thiele modulus $\phi_p = L_c\sqrt{k_m \rho_p / D_e}(n = 1)$

ε bed porosity, –

ε_p porosity of a catalyst particle, –

ε_l liquid hold-up, –

η_p effectiveness factor of a catalyst pellet –

η_{cw} effectiveness factor for a completely wetted slab, –

η_{hw} effectiveness factor for a half-wetted slab, –

η_{nw} effectiveness factor for a non-wetted slab, –

η_o overall effectiveness factor, –

ν absolute value of the stoichiometric coefficient for reactant A, –
ρ dimensionless coordinate inside the cylinder shell, –
ρ_i value of ρ at the inner surface of the cylinder shell, –
ρ_l liquid density, g l^{-1}
ρ_p density of a catalyst particle, g cat l^{-1}
ρ_s density of catalyst packing, g cat l^{-1}
τ tortuosity factor, –

References

[1] G. Valerius, X. Zhu and H. Hofmann, Modelling of trickle-bed reactors — extended definitions and new approximations, *Chem. Eng. Process.*, *35* (1996) 1–9.

[2] G. Valerius, Die Modellierung eines Rieselreaktors unter Berucksichtigung einer unvollständigen äußeren Benetzung des Katalysators, *Dissertation*, University of Erlangen, 1994.

[3] W.F. Linke and D. Seidell, *Solubilities of Inorganic and Organic Components*, Am. Chem. Soc., Washington, DC, 1965.

[4] E.G. Beaudry, M.P. Dudukovic and P.L. Mills, Trickle-bed reactors: liquid diffusional effects in a gas-limited reaction, *AIChE J.*, *33* (1987) 1435–1447.

[5] A. Burghardt, A.S. Kolodziej and M. Jaroszynski, Experimental studies of liquid–solid wetting efficiency in trickle-bed cocurrent reactors, *Chem. Eng. Prog.*, *28* (1990) 35–49.

[6] A.J. Colombo, G. Baldi and S. Sicardi, Liquid–solid contacting effectiveness in trickle-bed reactors, *Chem. Eng. Sci.*, *31* (1976) 1101–1108.

[7] P.L. Mills and M.P. Dudukovic, Evaluation of liquid–solid contacting in trickle-bed reactors by tracer methods, *AIChE J.*, *27* (1981) 893–904.

[8] J.G. Schwarz, E. Weger and M.P. Dudukovic, A new tracer method for determination of liquid–solid contacting efficiency in trickle-bed reactors, *AIChE J*, *22* (1976) 894.

[9] Z.E. Ring and R.W. Missen, Trickle-bed reactors: effect of wetting geometry on overall effectiveness factor, *Can. J. Chem. Eng.*, *64* (1986) 117.

[10] I.V. Yentekakis and C.G. Vayenas, Effectiveness factors for reactions between volatile and nonvolatile components in partially wetted catalysts, *Chem. Eng. Sci.*, *42* (1987) 1322–1332.

[11] A. Steitwieser and C.H. Heathcock, *Organische Chemie*, Verlag Chemie, Weinheim, 1980.

[12] A. Lakota and J. Levec, Solid–liquid mass transfer in packed beds with cocurrent downward two-phase flow, *AIChE J.*, *36* (1990) 1444–1448.

[13] C.N. Satterfield, Trickle-bed reactors, *AIChE J.*, *21* (1975) 209–228.

[14] S. Goto and J.M. Smith, Trickle-bed reactor performance. I. Holdup and mass transfer, *AIChE J.*, *21* (1975) 706–713.